BioCore Exploring Scientific Community

International Journal of Nanotechnology in Medicine & Engineering

ISSN 2474-8811

Research Article Open Access

Kinetic and Adsorption Studies of a Thiazine and Triarylmethane Dye onto Bamboo Impregnated Nanoscale Manganese

Solomon E. Shaibu*[1], Folahan A. Adekola[2], Halimat I. Adegoke[2], Olushola S. Ayanda[3]
[1]Department of Chemistry, University of Uyo, Uyo, Nigeria
[2]Department of Chemistry, University of Ilorin, Ilorin, Nigeria
[3]Department of Industrial Chemistry, Federal University Oye Ekiti, Ekiti State, Nigeria
Corresponding Author: Solomon E. Shaibu, Department of Chemistry, University of Uyo, Uyo, Nigeria.
Email: shaibusolomon@uniuyo.edu.ng

Citation: Solomon E. Shaibu et al. (2017), Kinetic and Adsorption Studies of a Thiazine and Triarylmethane Dye onto Bamboo Impregnated Nanoscale Manganese. Int J Nano Med & Eng. 2:9, 143-149. DOI:10.25141/2474-8811-2017-9.0156

Received: September 06, 2017; **Accepted:** September 19, 2017; **Published:** October 27, 2017

Abstract:
In this study, bamboo impregnated with nanoscale manganese (BMn) was prepared by the aqueous phase borohydride reduction method and characterized using scanning electron microscopy (SEM), Fourier transform infrared spectroscopy (FTIR) and PIXE analysis. The synthesized nMn-bamboo (BMn) was subsequently applied for the sorption of methylene blue (MB) and acid violet 19 (AV 19) from aqueous solution representing a thiazine and a triarylmethane class of dyes, respectively. Batch adsorptions of MB and AV 19 dyes were investigated under various experimental conditions such as pH, contact time, initial concentration of dyes and adsorbent dosage. The results showed that the synthesized BMn is an effective adsorbent with a high MB and AV 19 dyes adsorption capacity above 180 mg/L for both dyes. At concentration 120 mg/L, usage of 0.02 g of BMn resulted to 263.5 and 187.2 mg/g removal efficiency for MB and AV 19, respectively at 165 rpm for a period of 120 min and at a solution pH of 7.6. The equilibrium data were best represented by Freundlich isotherm model and the pseudo-second order kinetic model better explained the kinetic data

Keywords: Thiazine, Triarymethane, Nanoscale Manganese (nMn), Bamboo, Adsorption, Kinetics

Introduction:

A malaise that has captured the world's attention over the past 20 years is the spate of water pollution around the world with textile industry being one of the largest polluters globally; the second after agriculture (put reference) (www.un.org). The World Bank estimates that almost 20% of global industrial water pollution comes from the treatment and dyeing of textiles (www.un.org).

Industrial dyes are highly coloured synthetic organic substances with complex structures, high colour intensity and low biodegradability. They persist for long distances in flowing water, inhibit the biological activities of aquatic biota and generally impact negatively on the domestic and economic values of water bodies. The annual consumption of dyes has been on the increase globally due to their diverse applications. It is estimated that more than 10% of the total 7 x 10^5 metric tonnes of dyes produced annually finds their way into water bodies via direct discharge as aqueous effluents or loss during colouration processes (Balasubramanian, 2009).

Adsorption is established over the years to be a viable alternative among remediation methods for the treatment of dye contaminated wastewater owing to its cost efficiency, versatility, and ease of operation (Garg et al., 2003). Removal of dyestuffs from aqueous media particularly methylene blue (MB) and acid violet 19 (AV 19) has been experimented recently using palygorskite in sodium sulphide solution (Tian et al., 2016), polyaniline-Fe_3O_4 composite (Patil et al., 2016), apple waste (Hesas et al., 2013), rice waste (Mashhadi et al., 2016), NiO nanoparticle (Samiey and Farhadi, 2014), graphene oxide, and carbon nanotubes (Li et al., 2016), calcium alginate, activated carbon and their composite beads (Hassan et al., 2014) under various experimental conditions by a number of researchers with promising results in terms of high percentage removal, kinetics and thermodynamics.Yang, et al., 2016, recently reported the effective removal of MB from aqueous solutions using polyvinyl alcohol/graphene oxide composites as adsorbent after characterization with SEM, FTIR and TGA and also got a high adsorption capacity of 476.2 mg/g at 50% adsorbent dosage. Similarly, Chang et al., 2016 prepared Fe_3O_4/activated montmorillonite (Fe_3O_4/Mt) nanocomposite by coprecipitation method and subsequently evaluated the adsorption capacity of Fe_3O_4/Mt nanocomposite for MB with 99.47% removal within 25 min after elucidation of the morphology and structure of the prepared nanocomposite. The reusability of the Fe_3O_4/Mt was also investigated

after a number of usages with 83.37% colour removal.

This study evaluates the efficiency of bamboo impregnated nanoscale manganese (BMn) as an adsorbent for the removal of MB and AV 19 from aqueous solution representing thiazine and triarylmethane dyes, respectively. The effects of pH, contact time, initial dye concentration, temperature and adsorbent dosage on the adsorption capacity were investigated. The experimental data were also fitted into different equilibrium and kinetic models and deductions made.

Experimental

Chemicals and Reagents

Analytical grade manganese chloride (Minimum assay 99.9%, Tianjin Kermel, Hebei, China), sodium borohydride (BDH 95%, prd no. 30114, Sigma Aldrich, Diegem, Belgium), MB dye (BDH prd no. 340484B, Sigma Aldrich, Diegem, Belgium), absolute ethanol (BDH Analar, 95% UN No. 1097), hydrochloric acid (purity 37%, density 1.1kg/cm3, Riedel-deHaen, Buffalo, NY, USA) and sodium hydroxide (BDH prod. No. 30167, Sigma Aldrich, Diegem, Belgium) were used without further purification.

Adsorbent (Bamboo Impregnated Nanoscale Manganese) Preparation

The BMn was prepared by borohydride reduction method with $MnCl_2.H_2O$ and bamboo in the ratio 1:1. The bamboo was washed, dried at room temperature and then chopped into small pieces for easy grinding. The chopped bamboo was pulverized into very fine particles with the help of mortar and pestle and soaked in HCl solution for 4 hrs, washed several times with deionized water and finally dried at room temperature prior to impregnation with nanoscale manganese. A 1.979 g of the treated bamboo was weighed and added into a solution of 0.05 M $MnCl_4.H_2O$ in a beaker and stirred on a magnetic stirrer (model: J. W. Towers) for 2 hr to ensure thorough mixture of both materials and then poured into a three neck flask before addition of the borohydride solution. A 0.53 M $NaBH_4$ solution was added into the beaker containing the mixture of the bamboo and $MnCl_4.H_2O$ solution. After the complete addition of the borohydride solution, the resulting mixture was further stirred for another 30 min. The resulting precipitate was washed several times with ethanol and filtered through 0.45 µm millipore filter paper by vacuum filtration technique and was then oven dried at 50 ^{0}C overnight (Frost et al., 2010 and Yuvukmar et al., 2011).

Characterization of Bmn

The scanning electron micrographs (SEM) of bamboo, nMn and nMn-bamboo were viewed under a FEITM scanning electron microscope (Nova Nano SEM 230, FEI, Hillsboro, OR, USA). A 1.7 MV tandem pelletron accelerator (model 5SDH) was used to determine the concentrations of the elements present while fourier transform infrared spectroscopy (FTIR) absorption spectra were obtained using the potassium bromide (KBr) pellet method and recorded over the range 4000 – 400 cm-1 using Shimadzu FTIR-8400s.

Adsorption Studies

Batch dye removal experiments with the prepared BMn were carried out in 100 mL flasks under vigorous agitation at 165 rpm. The experiment involved preparing 50 mL of dye solutions with desired initial concentration and contacting with a known mass of the adsorbent (BMn) at a predefined time and speed. The pH of the solution was adjusted using 0.1 M HCl or 0.1 M NaOH solutions with a pH meter model (pH 211 microprocessor). A 0.02 g of BMn powder was added to the solution and the obtained suspension immediately agitated for 120 min. After the contact time elapsed, the suspension was centrifuged and the supernatant syringed and analyzed using a UV/visible spectrophotometer (UV/vis DU 730, Beckman Coulter, Pasadena, CA, USA) at maximum absorption wavelengths of 665 and 480 nm for MB and AV 19 dyes, respectively. The amount of MB and AV 19 adsorbed, qe (mg/g) was obtained using Equation 1:

$$q_e = \frac{(C_0 - C_f)V}{W} \qquad 1$$

where C_0 and C_f are the initial and final concentrations of dyes(mg/L), respectively, V is the volume of the solution (L) and W is the amount of adsorbent used (g).

All tests were performed in triplicates to ensure reproducibility; the mean of the measurements was reported. Furthermore, all experiments were performed at room temperature (29 ± 2 ^{0}C). The investigated ranges of the experimental variables were as follows: MB dye concentration 10 - 120 mg/L, initial pH of solution 3 – 11, adsorbent dosage 0.01- 0.05 g and contact time of 10 - 180 min.

Results and Discussion

Characterisation

The surface morphologies of BMn studied using SEM are shown in Figs 1a and b. It is observed that the surface of the BMn is non-uniform, rough and characterized with pores. Presence of deep fissures, numerous openings and folds on the surface of the bamboo fiber houses the manganese nanoparticles (nMn) and consequently leads to a synergistic adsorption and trapping of the dye molecules during the removal process.

FTIR spectra of bamboo, nMn and BMn in Fig. 2, show prominent absorption bands with a strong broad O-H, prominent C-H, non-conjugated C-O stretching and an aromatic skeletal vibration at around 3417.98 cm^{-1}, 2939.61 cm-1, 1728.28 cm^{-1} and 1604.83 cm^{-1}, respectively, which are attributed to the presence of the bamboo in the BMn matrix.

The concentration of elements present ranges from Si to Ni as shown in Table 1. Many of the elements detected had values above 4000 mg/L except for Ni, Ti, Ca and K which were below 500 mg/L. The concentrations of the Mn and Cl in BMn were evidently higher than other elements present at about 109879 and 46723 mg/L respectively due to the composition of the starting materials used for the preparation.

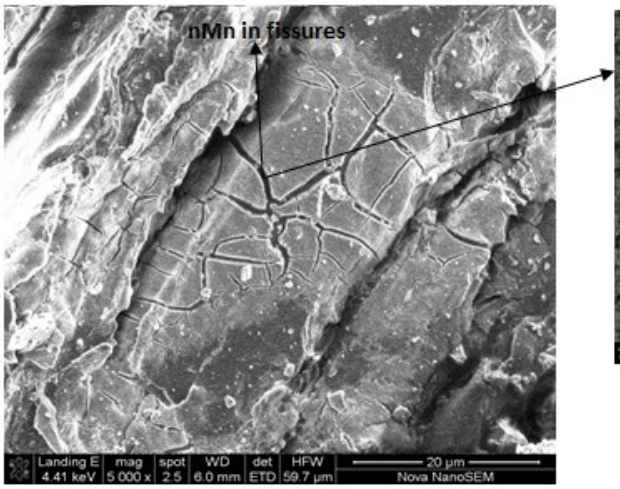

Fig. 1a: SEM of BMn

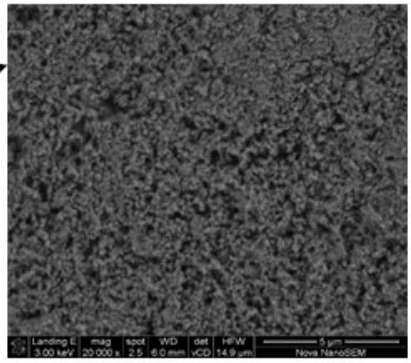

Fig. 1b: Inset of the SEM of BMn

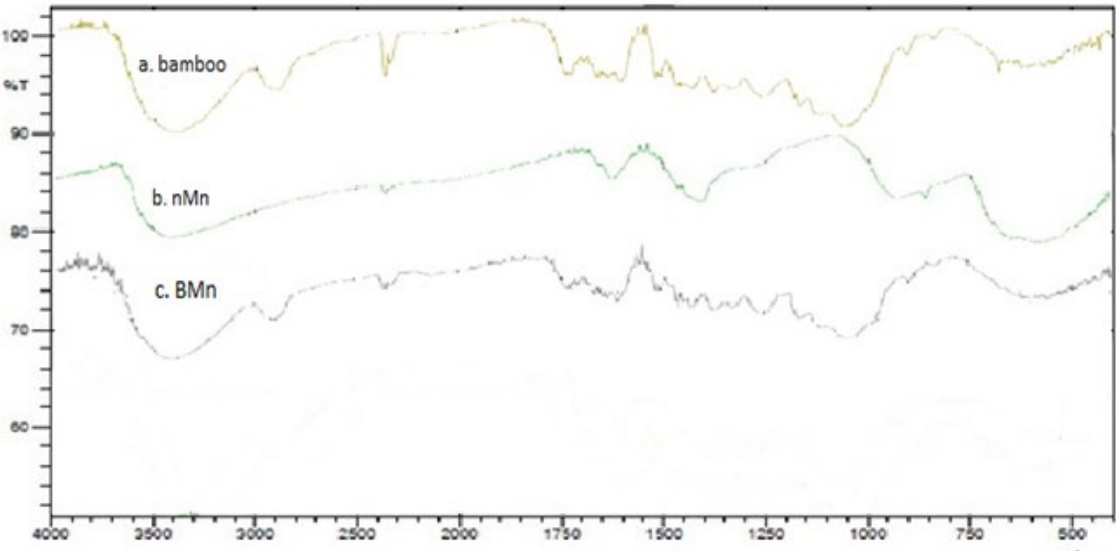

Fig. 2: FTIR spectra of bamboo, nanoscale manganese (nMn) and BMn

Table 1: Concentration of elements in BMn by PIXE analysis

Element	Concentration (mg/L)
Al	7369.7±217.33
Si	3485.9±153.64
Cl	46723.5±238.29
K	62.6±21.51
Ca	345.4±16.27
Ti	35.4±10.51
Mn	109879.9±164.82
Fe	4232.2±243.35
Ni	48.0±11.62

Effect of Initial Concentration

The initial dye concentration plays a vital role in surmounting the mass transfer resistance of the dyes between the aqueous and the solid phase. The quantity of dyes adsorbed per gram increased with increase in concentration for both MB and AV 19 (Fig 3), suggesting that at lower MB concentration, there were many vacant adsorption sites available for the dye molecules to attach to until the surface of the adsorbent was saturated at 120 mg/L where the amount of dyes adsorbed did not increase significantly. In addition, similar to the report by Aniba & Haris, 2010 and Samiey & Farhadi 2014, the sorption capacities of BMn increased from 23.071-252.91 mg/g and 15.2-187.2 mg/g for MB and AV 19, respectively as the initial concentration of the dyes increased from 10-120 mg/L.

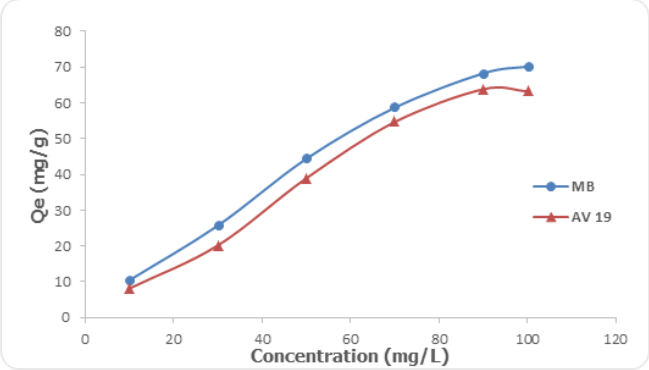

Fig. 3: Effect of Initial Concentration (m=0.02 g, time=120 min, pH=6.5 and T=28±2^{0}C)

Effect of Adsorbent Dosage

The effect of adsorbent dosage on MB and AV 19 adsorption is shown in Fig. 4. Removal efficiency decreased for both dyes as the amount of adsorbent increased. The quantity adsorbed of MB and AV 19 decreased from 275.6 and 198.42 mg/g to 102.3 and 91.34 mg/g as the amount of adsorbent increased from 0.01 to 0.05 g for MB and AV 19, respectively. At the outset of the adsorption process, BMn had higher mobility and access to the dye molecules but as the adsorbent dosage increased, overlapping or aggregation of adsorption sites must have occurred leading to a reduction in the total surface area available for the adsorption of MB and AV 19 dyes (Renugadevi et al., 2011).

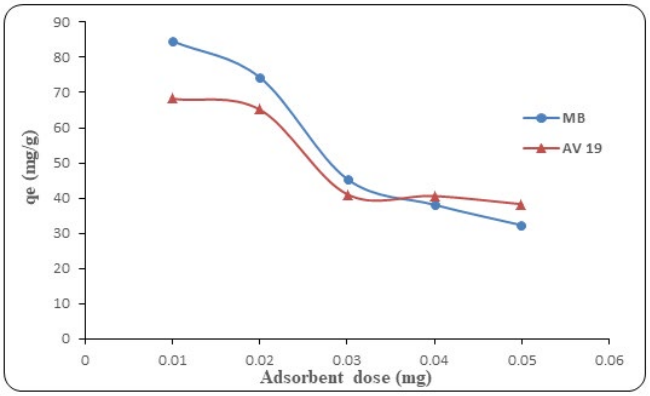

Fig. 4: Effect of Adsorbent Dosage (Co= 120 mg/L, time=120 min, pH=6.5 and T=28±2^{0}C)

Effect of Initial pH

The degree of electrostatic charges, stability and structure of dye molecules are controlled by the pH of the solution (Seow & Lim, 2016). This parameter affects the surface charge of the adsorbent, the degree of ionization of dyes and dissociation of functional groups on the active sites of the adsorbents (Ai et al., 2011).

As can be seen in Fig. 5, the adsorption of MB and AV 19 dyes onto BMn is highly dependent on the initial pH of solution. The amount of MB and AV 19 adsorbed increased from 31.2 to 183.4 mg/g with increase in solution pH from 3-5. No significant increase was noted until pH 9 where a rapid adsorption was observed from 201.6 to 252.3 mg/g.

This is ascribed to the presence of charged reactive group on the surface and also at acidic pH, hydrogen ion and other cations present in the solution may compete with dye ions for the vacant adsorption sites on the surface of BMn, thereby obstructing the adsorption of dyes. In alkaline environment, there are possibly more negative charges present on the adsorbent's surface, due to the deprotonation of the surface hydroxyl site, the number of ionisable sites on BMn increases and the adsorption of MB and AV 19 molecules with more negatively charged adsorbents can easily take place. This is similar to reports by Dhuha et al., 2012 and Hu et al., 2006.

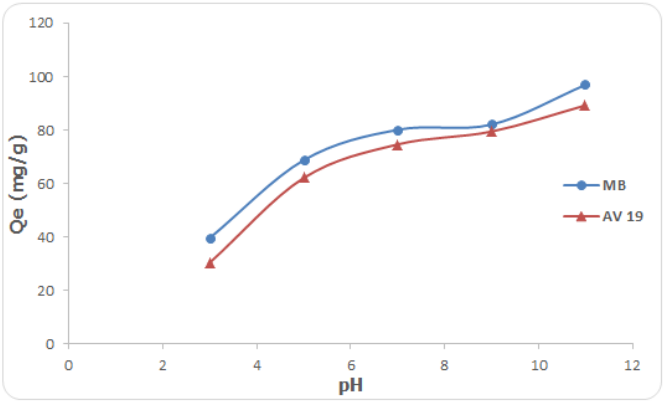

Fig. 5: Effect of pH (Co= 120 mg/L, m = 0.02 g, time=120 min, and T=28±2^{0}C)

Effect of Time

Generally, adsorption is faster at the initial stages of the process and slower as it approaches equilibrium. At the outset, large vacant surface sites are available on the surface of the adsorbent which becomes saturated with time and the remaining vacant surface sites become difficult to occupy due to the slow pore diffusion of the dye molecules and repulsive forces between the solid molecules and the bulk phases as it approaches equilibrium. This trend was observed for the adsorption of MB and AV 19 dyes as shown in Fig. 6, analogous to the study conducted by Bellir et al., 2010.

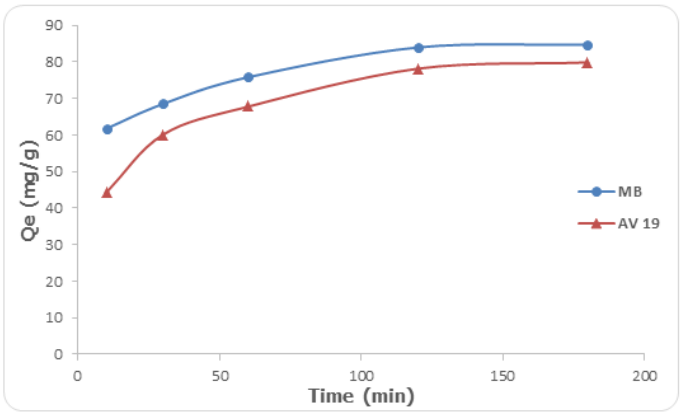

Fig. 6: Effect of Time (Co= 120 mg/L, m = 0.02 g, pH=6.5 and T=28±2^{0}C)

Adsorption Isotherm

Langmuir and Freundlich adsorption isotherm models were used to test the equilibrium data of MB and AV 19 adsorption onto BMn. The Langmuir equation (Eq. 2), which is a widely used model, is valid for monolayer sorption on a surface containing a finite number of adsorption sites, predicting a homogeneous distribution of sorption energies while the heterogeneity of adsorption sites and sorption energy are deduced from Freundlich equation. This equation is also applicable to multilayer adsorption (Eq. 3).

$$\frac{C_e}{q_e} = \frac{1}{Q_0 b} + \left(\frac{1}{Q_0}\right) C_e \qquad 2$$

$$\log q_e = \log K_F + \left(\frac{1}{n}\right) \log C_e \qquad 3$$

where Ce is the equilibrium concentration of the adsorbate (mg/L), qe the amount of adsorbate adsorbed per unit mass of adsorbate (mg/L), Qo and b are Langmuir constants related to adsorption capacity and rate of adsorption, respectively. KF and n are Freundlich constants, n is an indication of how favourable the adsorption process and KF is the adsorption capacity of the adsorbent.

Table 2: Isotherm parameters for the adsorption of MB and AV 19 onto BMn

ISOTHERM	PARAMETERS	VALUES	
		MB	AV 19
Freundlich	K_f(mg/g(L/mg)$^{1/n}$)	2.6778	2.333
	n	1.3348	2.717
	R^2	0.986	0.982
Langmuir	Q_o (mg/g)	500	200
	b (L/mg)	0.002	0.008
	R^2	0.968	0.974

The data for the adsorption of MB and AV 19 onto BMn fitted more to Freundlich isotherm as shown in Fig. 7 with regression coefficient of 0.986 and 0.982, respectively. This indicates that the dyes are physisorbed on the surface of the adsorbent. The good agreement of Freundlich's isotherm with the adsorption data may be due to heterogeneous distribution of active sites on BMn. The model (Eq. 2) assumes the surface of adsorbents to be non-uniform and characterized by multilayer adsorption. The Freundlich constant n (1.3348) indicates that the adsorption is favorable. However, Langmuir isotherm (Fig. 8) poorly interpretes the adsorption data for MB and AV 19 with a regression coefficients of 0.185 and 0.278, respectively.

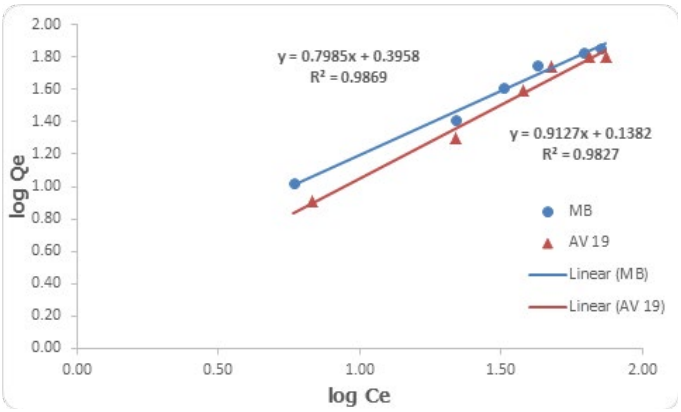

Fig. 7 : Freundlich Isotherm

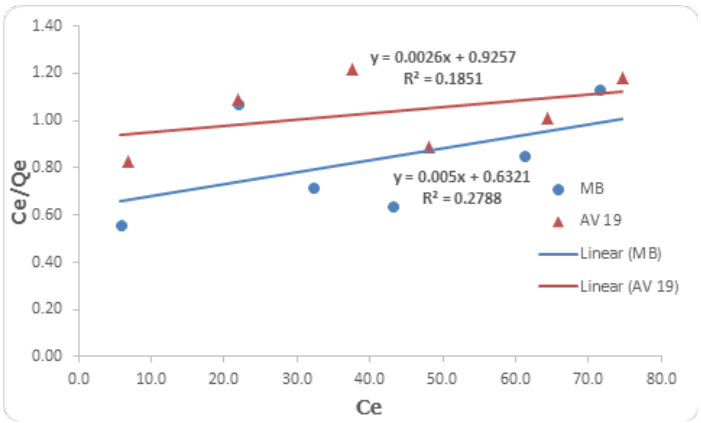

Fig. 8 : Langmuir Isotherm

Kinetic Models

To study the kinetics of the adsorption of MB and AV 19 onto BMn, three different kinetic models were used for the analysis of the data of each of the adsorbents, viz: pseudo-first order, pseudo-second order and Elovich models.

Evidently, the adsorption data fitted more to the pseudo-second order with a regression coefficient of 0.9995 and 0.998 for MB and AV 19, respectively as shown in Figs. 9a – 9c and Table 3.

Table 3: Kinetic parameters and correlation coefficients of the adsorption of MB and AV 19 onto BMn

MODELS	PARAMETERS	VALUES	
		MB	AV 19
Pseudo-first order	K_1 [min^{-1}]	0.0299	0.0253
	$Q_{e,cal}$ [mg/l]	40.086	49.204
	R^2	0.965	0.985
Pseudo-second order	K_2 [$g.mg^{-1}.min^{-1}$]	0.002	0.001
	$Q_{e,cal}$ [mg/l]	90.91	83.33
	R^2	0.9995	0.998
Elovich			
	β [g.min/mg]	0.1168	0.0791
	α [$g.min^2.mg$]	1.7522	1.105
	R^2	0.979	0.990

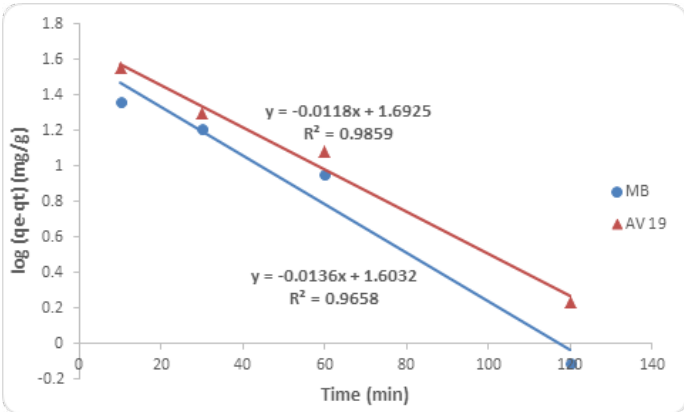

Fig. 9a: Pseudo-first order`

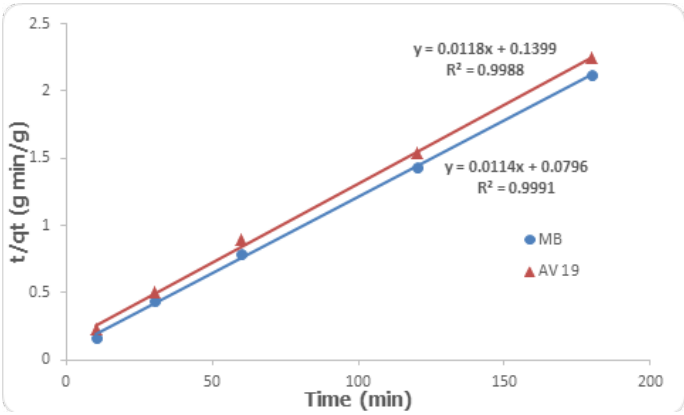

Fig. 9b: Pseudo second order

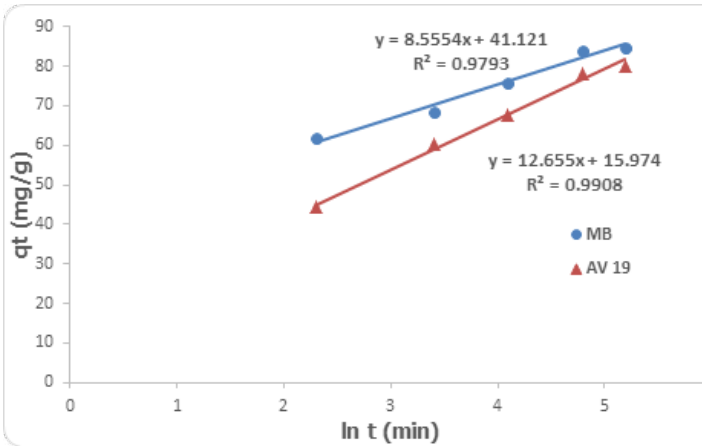

Fig. 9c: Elovich

Conclusion

This study confirmed that the nMn-bamboo prepared by the borohydride reduction method was effective for the removal of MB and AV 19 dyes from aqueous solution. The results showed that the adsorption is highly influenced by the initial concentration, solution's pH, adsorbent dosage and contact time. The adsorption data were adequately interpreted by Freundlich adsorption isotherm while the kinetic data were better explained by pseudo-second order kinetic model.

Acknowledgement

Sincere appreciation goes to the co authors for their invaluable contributions

References

1. Ai L., Zhang C., Liao F., (2011). Removal of methylene blue from aqueous solution with magnetite loaded multi-wall carbon nanotube: kinetic, isotherm and mechanism analysis. Journal of hazardous materials, 198, 282-290.

2. Aniba M. and Hariri S.A., (2010) Removal of methylene blue from aqueous using nanoporous SBA-3. Desalination, 261(1-2); 61-66.

3. Balasubramanian, N. (2009). Electrochemical degradation of remazol Black B dye effluent. Clean Soil Air Water, 37, (11):889–900.

4. Bellir, K., Mossab B. L, & Meniai A-Hassen. (2010). Removal of Methylene Blue from aqueous solutions using an Acid Activated Algerian Bentonite: Equilibrium and Kinetic Studies. International Renewable Energy Congress 361-367.

5. Chang, J., Ma, J., Ma, Q., Zhang, D., Qiao, N., Hu, M., & Ma, H. (2016). Adsorption of methylene blue onto Fe 3 O 4/activated montmorillonite nanocomposite. Applied Clay Science, 119, 132-140.

6. Dhuha D.S., Wisam S.U. and Tariq N.M. (2012). Determination the Optimal Conditions of Methylene Blue Adsorption by the Chicken Egg Shell Membrane. International Journal of Poultry Science, 11 (6): 391-396.

7. Frost, R. L., Xi, Y. and He, H.(2010). Synthesis, characterization of palygorskite supported zero-valent iron and its application for methylene blue adsorption. Journal of Colloid and Interface Science, 341, 153-161.

8. Garg V.K. Gupta R. Yadav B. and Kumar R, (2003). Removal of acid dyes by low cost adsorbent. Bioresource Technology, 89, 121-124.

9. Hassan, A. F., Abdel-Mohsen, A. M., & Fouda, M. M. (2014). Comparative study of calcium alginate, activated carbon, and their composite beads on methylene blue adsorption. Carbohydrate polymers, 102, 192-198.

10. Hesas, R. H., Arami-Niya, A., Daud, W. M. A. W., & Sahu, J. N. (2013). Preparation and characterization of activated carbon from apple waste by microwave-assisted phosphoric acid activation: application in methylene blue adsorption. BioResources, 8(2), 2950-2966.

11. Hu Q.H., Qiao S.Z. and Haghseresht F. (2006). Adsorption study for the removal of basic red dye using bentonite. Ind. Eng. Chem. Res. 45(1), 733-738.

12. Li, Y., Du, Q., Liu, T., Peng, X., Wang, J., Sun, J.,& Xia, L. (2013). Comparative study of methylene blue dye adsorption onto activated carbon, graphene oxide, and carbon nanotubes. Chemical Engineering Research and Design, 91(2), 361-368.

13. Mashhadi, S., Javadian, H., Ghasemi, M., Saleh, T. A., & Gupta, V. K. (2016). Microwave induced H2SO4 activation of activated carbon derived from rice agricultural wastes for sorption of methylene blue from aqueous solution. Desalination and Water Treatment, 1-14.

14. Patil, M. R., Khairnar, S. D., & Shrivastava, V. S. (2016). Synthesis, characterisation of polyaniline–Fe3O4 magnetic nanocomposite and its application for removal of an acid violet 19 dye. Applied Nanoscience, 6(4), 495-502.

15. Renugadevi, N., Sangeetha, R., & Lalitha, P. (2011). Kinetics of the adsorption of methylene blue from an industrial dyeing effluent onto activated carbon prepared from the fruits of Mimusops Elengi. Archives of Applied Science Research, 3(3), 492-498.

16. Samiey, B., & Farhadi, S. (2014). Kinetics and thermodynamics of adsorption of fuchsin acid on nickel oxide nanoparticles. Acta Chimica Slovenica, 60(4), 763-773.

17. Seow, T. W., & Lim, C. K. (2016). Removal of Dye by Adsorption: A Review. International Journal of Applied Engineering Research, 11(4), 2675-2679.

18. Tian, G., Wang, W., Kang, Y., & Wang, A. (2016). Palygorskite in sodium sulphide solution via hydrothermal process for enhanced methylene blue adsorption. Journal of the Taiwan Institute of Chemical Engineers, 58, 417-423.

19. www.un.org. Transforming our world: the 2030 Agenda for Sustainable Development. retrieved 22-02-2016.

20. Yang, X., Li, Y., Du, Q., Wang, X., Hu, S., Chen, L., & Xia, L. (2016). Adsorption of methylene blue from aqueous solutions by polyvinyl alcohol/graphene oxide composites. Journal of Nanoscience and Nanotechnology, 16(2), 1775-1782.

21. Yuvakkumar R., Elango V., Rajendran V., Kannan N., (2011). Preparation and characterization of zero-valent iron manoparticles. Digest Journal of Nanomaterials and biostructures, 6(4); 1771-1776.